Plant Gene 10 (2017) 17–25

Contents lists available at ScienceDirect

Plant Gene

journal homepage: www.elsevier.com/locate/plantgene

Isolation and characterization of a floral homeotic gene in *Fraxinus nigra* causing earlier flowering and homeotic alterations in transgenic *Arabidopsis*

Jun Hyung Lee[a], Paula M. Pijut[b,*]

[a] Purdue University, Dept. of Forestry and Natural Resources, Hardwood Tree Improvement and Regeneration Center (HTIRC), 715 West State St., West Lafayette, IN 47907, United States

[b] USDA Forest Service, Northern Research Station, HTIRC, 715 West State St., West Lafayette, IN 47907, United States

ARTICLE INFO

Keywords:
AGAMOUS
Black ash
Ectopic expression
Flowering
Fraxinus nigra
MADS

ABSTRACT

Reproductive sterility, which can be obtained by manipulating floral organ identity genes, is an important tool for gene containment of genetically engineered trees. In *Arabidopsis*, *AGAMOUS* (*AG*) is the only C-class gene responsible for both floral meristem determinacy and floral organ identity, and its mutations produce sterility. As a first step in an effort to develop transgenic sterile black ash (*Fraxinus nigra*), an *AG* ortholog in black ash (*FnAG*) was isolated using reverse transcription polymerase chain reaction and rapid amplification of cDNA ends. Analysis of the deduced amino acid sequence showed a typical MIKC structure of type II plant MADS-box protein with a highly conserved MADS-domain. Phylogenetic analysis revealed that *FnAG* had a close relationship with *AG* orthologs from other woody species. *FnAG* transcript was mainly expressed in reproductive tissues, but rarely detected in the vegetative tissues, consistent with the ABC model for floral development. A functional analysis was performed by ectopic expression of *FnAG* driven by the CaMV 35S promoter in transgenic *Arabidopsis*. Transformed plants showed homeotic conversions of carpeloid sepals and stamenoid petals. Curled leaves, reduced plant size, and earlier flowering were also observed in transgenic *Arabidopsis*. These data indicated that the *FnAG* functions in the same way as *AG* in *Arabidopsis*. These results provide the framework for targeted genome editing of black ash, an ecologically and economically important wetland species.

1. Introduction

Black ash (*Fraxinus nigra* Marsh.) is an economically and ecologically important hardwood species in northeastern North America. The wood is used for cabinets, paneling, flooring, and is preferred by Native Americans for making splints for basketry (Benedict, 2001; Beasley and Pijut, 2013). Black ash also provides food and habitat for wildlife (Leopold et al., 1998) and this species has a great ecological impact, especially in riparian ecosystems (Nisbet et al., 2015). Black ash flowers are perfect or dioecious; they occur in panicles that arise from leaf scar axils produced the previous year (Gucker, 2005). The flowers appear before the leaves.

Emerald ash borer (EAB; *Agrilus planipennis*), an invasive wood-boring beetle from Asia, threatens all North American ash species including black ash with devastating economic and ecological impacts (Poland and McCullough, 2006; Kovacs et al., 2011). In order to manage this aggressive pest and conserve *Fraxinus* spp., there have been numerous calls for genetically engineered ash trees resistant to the EAB. Concerns about transgene flow and its potential impact on the environment, however, limit the widespread acceptance and regulatory approval of transgenic trees (van Frankenhuyzen and Beardmore, 2004). Reproductive sterility, obtained by disrupting flower development, is one of several efficient strategies for gene containment in transgenic crops and trees (Daniell, 2002; Brunner et al., 2007).

Previous studies in model plants established the well-known ABC model to describe the genetic mechanism regulating flower development (Schwarz-Sommer et al., 1990; Coen and Meyerowitz, 1991; Meyerowitz et al., 1991). This model proposed that three classes of homeotic genes act in combination to control floral organ identity: A-class alone controls the formation of sepals; A- and B-classes trigger petal development; B- and C-classes regulate the formation of stamens; and C-class alone directs the formation of carpels. The ABC model has been extended by adding D-class for ovule development (Angenent et al., 1995) and E-class which was required for petal, stamen, and carpel development (Pelaz et al., 2000; Honma and Goto, 2001). According to the ABCDE model, MADS-box proteins interact with DNA to form multimeric complexes that regulate the development of different floral organs (Honma and Goto, 2001).

MADS-box genes are a superfamily of transcription factors found in fungi, animals, and plants. They are distinguished as type I and type II

* Corresponding author.
E-mail addresses: ppijut@fs.fed.us, ppijut@purdue.edu (P.M. Pijut).

http://dx.doi.org/10.1016/j.plgene.2017.03.003
Received 2 December 2016; Received in revised form 6 March 2017; Accepted 17 March 2017
Available online 18 March 2017
2352-4073/ Published by Elsevier B.V.

(Alvarez-Buylla et al., 2000; Gramzow et al., 2010). The type II MADS-box genes in plants encode MIKC-type proteins that consist of four domains: a highly conserved MADS (M) domain for DNA binding; an intervening (I) domain for the selective formation of DNA-binding dimers; a keratin (K) domain for the formation of an amphipathic helix that promotes protein-protein interaction; and the most variable region, the C-terminal (C) domain, the function of which is not yet known (Theissen et al., 2000). There are around 100 MADS-box genes in flowering plants, but *AGAMOUS* (*AG*) is the only C-class gene found in *Arabidopsis*. A flower of the *Arabidopsis ag* mutant shows petals and new flowers instead of stamens and carpels, respectively, while overexpression of *AG* induces homeotic changes of sepals to carpels, and petals to stamen (*apetala2* (*ap2*)-like phenotype) indicating that *AG* was involved in both floral meristem determinacy and floral organ identity (Yanofsky et al., 1990; Mizukami and Ma, 1992). *AG* homologs have been isolated and studied in a variety of species including woody plants, such as poplar (Brunner et al., 2000), black cherry (Liu et al., 2010), green ash (Du and Pijut, 2010), radiata pine (Liu, 2012), London plane tree (Zhang et al., 2013), and pecan (Zhang et al., 2016). Ectopic expression of *AG* homologs in transgenic plants resulted in homeotic conversion of sepals and petals into carpels and stamens, respectively, which confirmed their function as a C-class floral organ identity gene (Benedito et al., 2004; Du and Pijut, 2010; Wang et al., 2012; Liu et al., 2013; Zhang et al., 2016). *AG* homologs from black ash have not been described.

In the present study, an *AG* ortholog from black ash (*FnAG*) was isolated and characterized as a first step to achieve gene containment in transgenic black ash. Functional homology to *AG* was tested by ectopic expression of *FnAG* in *Arabidopsis thaliana* (with *ap2*-like phenotype in the two outer floral whorls).

2. Materials and methods

2.1. Plant materials

Flowers and leaves were collected in April 2014 from mature male and female *Fraxinus nigra* trees at the Purdue Wildlife Area, Purdue University, and the Ross Hills Park, West Lafayette, IN, USA. Leaves and stems from in vitro shoot cultures of black ash maintained as described by Beasley and Pijut (2013) were also collected for RNA extraction. Samples were immediately frozen in liquid nitrogen and stored at − 80 °C until used for analysis.

Arabidopsis thaliana Col-0 ecotype seeds were obtained from the Arabidopsis Biological Resource Center (ABRC) at The Ohio State University, Columbus, OH, USA. Seeds were stratified for 3 days at 4 °C in the dark to break seed dormancy, and then sown onto Murashige and Skoog (1962) (MS; M499, PhytoTechnology Laboratories, Shawnee Mission, KS) medium supplemented with 10 g L^{-1} sucrose, 0.5 g L^{-1} 2-morpholinoethanesulfonic acid (MES), 8 g L^{-1} Bacto agar, pH 5.7 in 150 × 15 mm petri dishes. Seeds germinated on agar medium were incubated at 25 °C under a 16 h photoperiod (~100 μmol m^{-2} s^{-1}) provided by cool-white fluorescent bulbs. The germinated seedlings were grown for 2 weeks, and then transferred to water-saturated soil in pots covered with a plastic film to maintain high humidity and placed in the greenhouse under long-day conditions. The plastic film was removed after 2 days.

2.2. Isolation of an AG ortholog from black ash

Total RNA was extracted from the leaves of in vitro shoot cultures using the RNeasy Plant Mini Kit (Qiagen, Valencia, CA, USA) according to manufacturer's instructions. Re-suspended RNA was treated with DNase I (Thermo Fisher Scientific, Grand Island, NY, USA) in order to remove genomic DNA, and the first-strand cDNA was synthesized from 1 μg total RNA using SuperScript III First-Strand Synthesis System (Thermo Fisher Scientific) and an oligo-dT primer. Degenerate primers AGP1 and AGP2 (Table 1) were designed based on other *AG* nucleotide sequences to amplify the internal fragment spanning part of the MADS-domain and the K-domain (Du and Pijut, 2010). Reverse transcriptase polymerase chain reaction (RT-PCR) was performed with a 25 μl PCR mixture containing 2.5 μl 10 × PCR buffer (5 PRIME, Gaithersburg, MD, USA), 1 μl 10 mM dNTP, 1 μl 10 μM AGP1 and AGP2 primers, respectively, 2 μl cDNA, and 0.25 μl 5 U μl^{-1} Taq polymerase (5 PRIME). The cycling program consisted of an initial denaturation at 94 °C for 2 min, followed by five cycles of 94 °C for 30 s, 42 °C for 30 s, 72 °C for 1 min, 35 additional cycles of 94 °C for 30 s, 47 °C for 30 s, 72 °C for 1 min, and a final extension at 72 °C for 10 min. A single strong band of expected size (258-bp) was purified with QIAquick Gel Extraction Kit (Qiagen), and was then cloned into pGEM-T Easy vector (Promega, Fitchburg, WI, USA) for sequencing at the Purdue University Genomic Center (West Lafayette, IN, USA). Based on the partial internal sequence of *FnAG*, two sets of gene specific primers were designed to perform 5′- and 3′-rapid amplification of cDNA ends (RACE) (First-Choice RLM-RACE; Life Technologies, Grand Island, NY, USA). For the first-round PCR, AGP3 and AGP4 (Table 1) were used as 5′- and 3′-RACE outer primers, respectively. For the second-round PCR, AGP5 and AGP6 (Table 1) were used as 5′- and 3′-RACE inner primers, respectively. The obtained fragments from the second round PCR were cloned into pGEM-T Easy vectors for sequencing, and then assembled to determine the full-length cDNA sequence. To amplify a complete coding sequence (CDS) and genomic sequence of *FnAG*, the first-strand cDNA and genomic DNA were used as a template, respectively, for PCR using AGP7 and AGP8 (Table 1) as forward and reverse primers, respectively. Unless noted otherwise, all PCR reactions were performed using Phusion High-Fidelity DNA polymerase (New England Biolabs, Ipswich, MA, USA) according to manufacturer's instructions for PCR mixture preparations, and all the cycling programs consisted of an initial denaturation at 98 °C for 30 s, followed by 35 cycles of 98 °C for 10 s, 58 °C for 30 s, 72 °C for 1 min, and a final extension at 72 °C for 10 min. The gene structure was determined by aligning the CDS and genomic DNA sequence of *FnAG*.

Table 1
Primer sequences.

Primer	Sequence (5′ - 3′)
AGP1	GGA TCG ARA ACA CVA CAN AYC G
AGP2	GYY TCT TGY TGG TAR WAC TG
AGP3	TGA GGA ATC TGA GCA GGC TTT C
AGP4	CGT CAG GTC ACT TTC TGT AAG C
AGP5	GAC ACT GTC GTT GGC ATA TTC A
AGP6	CTT GCT CAA GAA GGC CTA TGA A
AGP7	ATG GCA TTG CAG AGT GAT CA
AGP8	TCA GAC TAA TTG AAG AGG TGG C
AtAG1	AGG CAA TTG ATG GGT GAG AC
AtAG2	TGG ATC GGA TTC GGG TAA TA
AtActin1	GTC GTA CAA CCG GTA TTG TGC TG
AtActin2	CCT CTC TCT GTA AGG ATC TTC ATG AG

2.3. Phylogenetic analyses

The deduced amino acid sequence of *FnAG* was used to search for *AG* homologs from other plants by BLASTX, and then all sequences were aligned by ClustalW (Larkin et al., 2007). A phylogenetic tree was constructed using the neighbor-joining method in MEGA5 software (Tamura et al., 2011). Bootstrap values were derived from 1000 replicate runs. GenBank accession numbers of amino acid sequences used were as follows: GAG2 (Q40872; *Panax ginseng*), CaMADS (ADU56831; *Coffea arabica*), NAG1 (Q43585; *Nicotiana tabacum*), NbAG (AFK13159; *N. benthamiana*), CaAGL2 (ADP06386; *Capsicum annuum*), pMADS3 (Q40885; *Petunia hybrida*), SiAG (AIS82595; *Sesamum indicum*), CsAG (ADP02394; *Citrus sinensis*), FpAG (AFP99884; *F. pennsylvanica*), VvAG (NP_001268097; *Vitis vinifera*), *AGAMOUS* (× 53579; *A.*

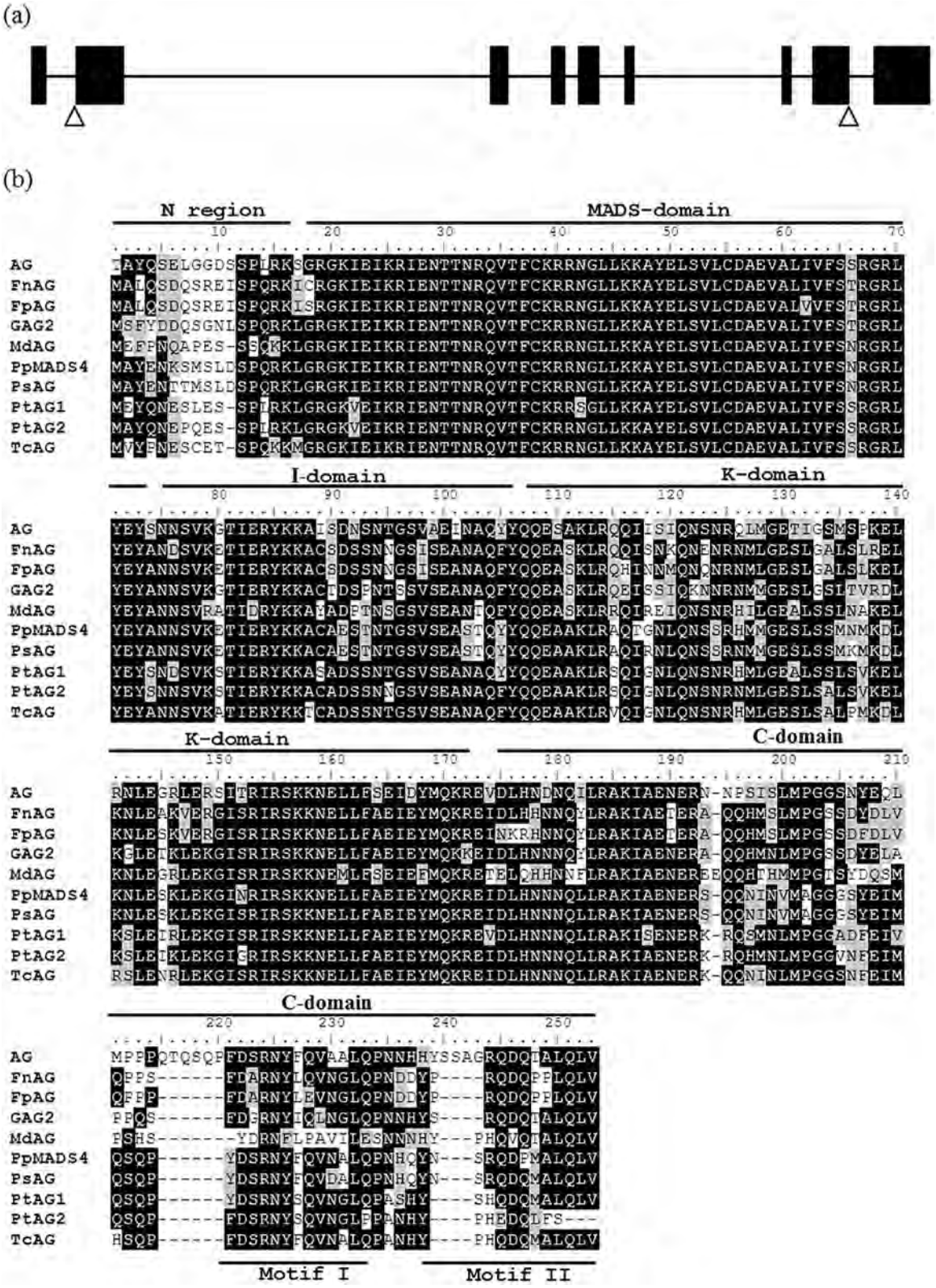

Fig. 1. Gene structure and deduced amino acid sequence alignment of an *AGAMOUS* ortholog in black ash (*FnAG*). (a) *FnAG* gene structure. Exons are depicted as *black boxes* and introns by *lines*. The *triangles* represent the position of start and stop codons. (b) Alignment of deduced amino acid sequences encoded by *FnAG* with *AG* homologs from a range of woody plant species. Identical amino acid residues in relation to *FnAG* are *black* and conserved residues are in *gray*. *Dots* indicate gaps inserted for alignment optimization. The amino acid terminal extension (N), MADS, intervening (I), keratin-like (K), and carboxyl terminal (C) regions are marked. Motifs I and II within the C region were indicated.

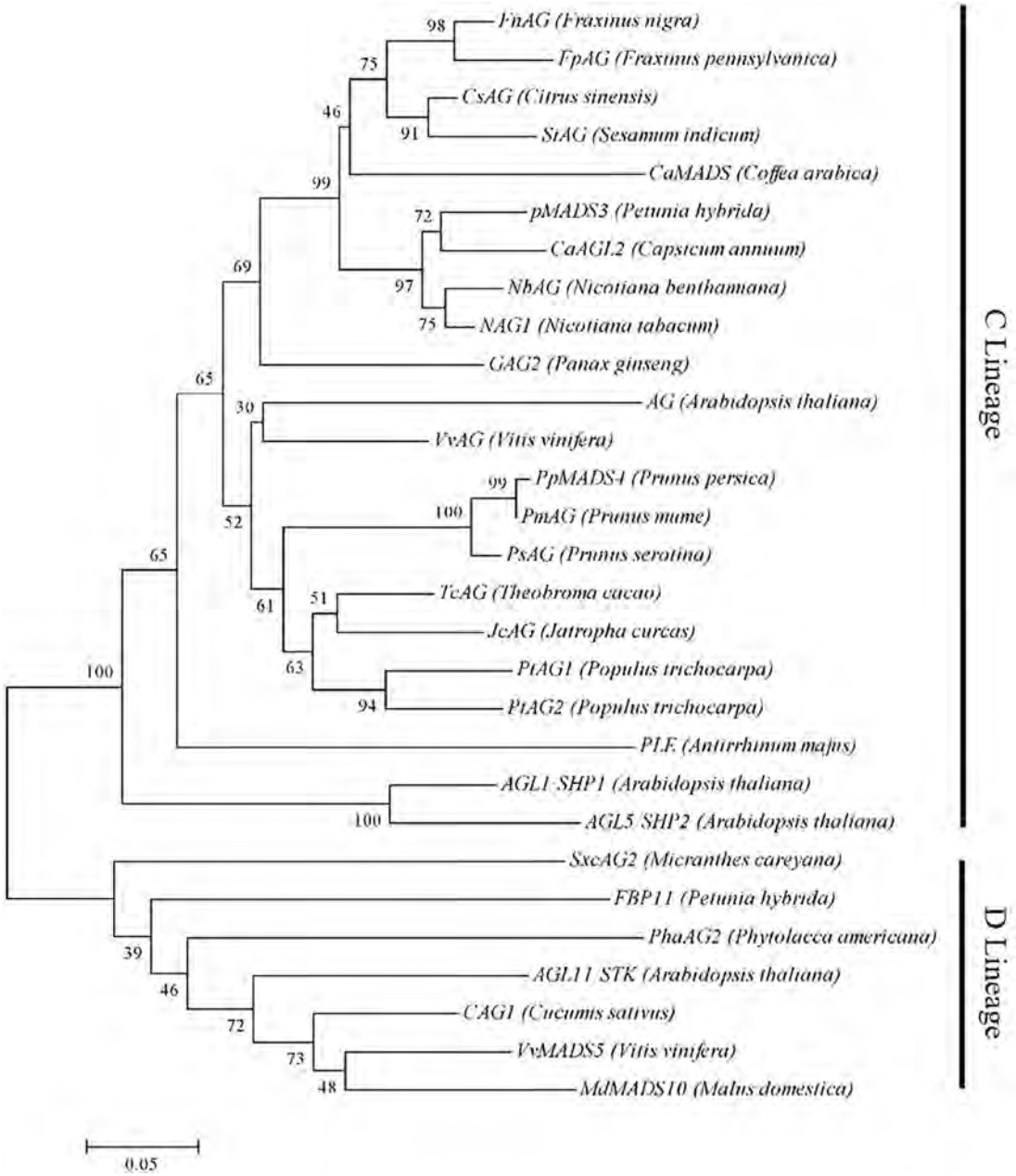

Fig. 2. Phylogenetic analysis of MADS-box proteins by the neighbor-joining method. The bootstrap confidence values (%) from 1000 replicates are indicated on the *branches*. The *scale at the bottom* indicates genetic distance proportional to the amino acid substitutions per site.

thaliana), JcAG (NP_001292936; *Jatropha curcas*), PtAG1 (AF052570; *Populus trichocarpa*), PtAG2 (AF052571; *P. hybrida*), TcAG (XP_007025251; *Theobroma cacao*), PsAG (EU938540.1; *P. serotina*), PpMADS4 (AAU29513; *P. persica*), PmAG (ABU41518; *P. mume*), PLE (BAI68391; *Antirrhinum majus*), AGL1/SHP1 (AEE79831.1; *A. thaliana*), AGL5/SHP2 (AEC10175.1; *A. thaliana*), FBP11 (CAA57445.1; *Petunia hybrida*), VvMADS5 (AAM21345.1; *V. vitis*), MdMADS10 (NP_001280931.1; *Malus domestica*), AGL11/STK (AEE82819.1; *A. thaliana*), CAG1 (NP_001267506.1; *Cucumis sativus*), PhaAG2 (AAS45706.1; *Phytolacca americana*), and SxcAG2 (AAS45704.1; *Micranthes careyana*).

2.4. Expression analysis of FnAG in black ash

To analyze the relative expression of *FnAG*, semi-quantitative RT-PCR and real-time PCR (qPCR) were performed. Total RNAs were extracted from vegetative tissues (leaves and in vitro shoot cultures) and reproductive tissues (male and female flowers) of black ash using the RNeasy Plant Mini Kit (Qiagen). DNase I (Thermo Fisher Scientific) treated RNA was then used in RT-PCR to synthesize first-strand cDNA using SuperScript III First-Strand Synthesis System (Thermo Fisher Scientific) and an oligo-dT primer. The qPCR was performed with 20 µl reaction solution containing 1 µl cDNA, 10 µM AGP3 and AGP6, and iTaq™ Universal SYBR® Green Supermix (Bio-Rad, Hercules, CA, USA). The cycling conditions consisted of DNA polymerase activation at 95 °C for 60 s, 40 cycles of 95 °C for 10 s, 57 °C for 20 s, 72 °C for 30 s, and followed by a melting curve analysis from 65 to 95 °C performed with the CFX Connect™ Real-Time PCR Detection System (Bio-Rad). Relative transcript levels for mRNAs were obtained using the comparative cycle threshold (C_t) method and normalized to translation elongation factor alpha (*eEFAα*) from black ash (Rivera-Vega et al., 2012). Each reaction had three biological replicates and was repeated twice.

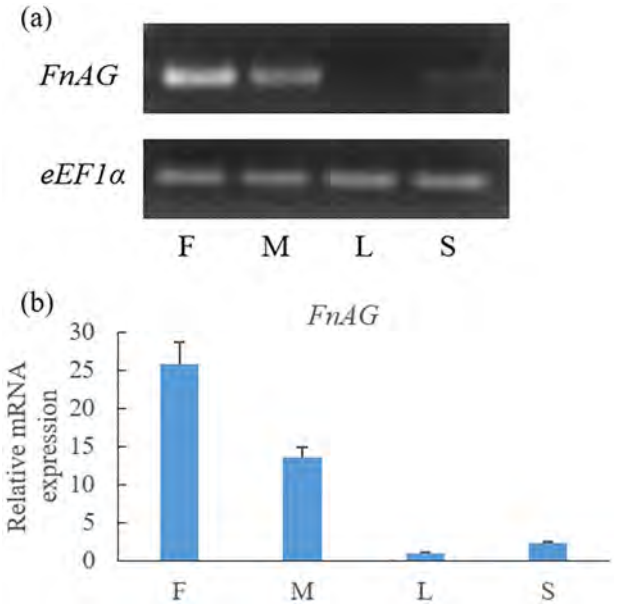

Fig. 3. Expression pattern of *FnAG* in various tissues of black ash by (a) Semi-quantitative RT-PCR analysis and (b) real-time PCR analysis. F, female flowers; M, male flowers; L, leaves; and S, in-vitro shoot cultures. The translation elongation factor alpha (*eEF1α*) gene was used as a constitutively expressed control. Each reaction had three biological replicates and was repeated two times. Error bars represent the standard deviation.

2.5. Functional analysis of FnAG through transformation of Arabidopsis thaliana

A binary vector pBI121 was used for *FnAG* insertion and over-expression in *Arabidopsis*. The GUS gene in pBI121 was replaced by the CDS sequence of *FnAG* which was driven by the CaMV 35S promoter. The *35S*::*FnAG* construct and the empty pBI121 vector as a control were transformed into *Agrobacterium tumefaciens* strain GV3101 by electroporation (Mattanovich et al., 1989), and then introduced into the wild-type *A. thaliana* ecotype Col-0 via the floral dip method (Zhang et al., 2006). T_1 seeds were placed onto agar plates containing MS medium with 50 mg L^{-1} kanamycin as selection agent. The seedlings were screened for 2–3 weeks on the plate and then kanamycin-resistant lines were transferred to water-saturated soil in pots. The integration of *FnAG* in the transgenic lines was confirmed by PCR using AGP3 and AGP4 primers. The number of days from planting to the first flower and the number of rosette leaves at that stage were recorded in T_3 plants. Statistical differences were assessed via analysis of variance with the SAS® 9.3 software package (SAS® Institute Inc., 2011).

2.6. Expression analysis of AtAG and FnAG in transgenic Arabidopsis

Floral tissues were collected from seven transgenic lines and wild-type *Arabidopsis*. The qPCR was performed as previously described. Primers, AtAG1 and AtAG2 (Table 1) were designed to amplify endogenous *AG*, and AGP3 and AGP6 were used to amplify ectopically expressed *FnAG*. Relative transcript levels for mRNAs were obtained using the C_t method and normalized to *ACTIN2* from *Arabidopsis* (AtActin1 and AtActin2 as forward and reverse primers, respectively). Each reaction had three biological replicates and was repeated twice.

3. Results

3.1. Isolation and sequence analysis of an AG ortholog from black ash

In order to isolate the *AG* ortholog from black ash, RT-PCR was performed using degenerate primers developed based on highly conserved sequence from a total of 17 *AG* homologs. An expected 258-bp internal fragment was amplified and sequenced (data not shown) to design specific primers for RACE. The results of 5′- and 3′-RACE revealed that *FnAG* cDNA was 1022-bp in length with a 5′ untranslated region (UTR) of 67-bp and a 3′ UTR of 226-bp upstream of the poly(A) tail. A 4578-bp genomic sequence was obtained and the alignment analysis of cDNA and genomic sequence showed that *FnAG* consisted of nine exons and eight introns (Fig. 1a). *FnAG* encodes a putative type II plant MADS-box protein of 242 amino acids containing N-, MADS-, I-, K-, and C-domains. It also contains two short, highly conserved regions, called *AG* motif I and *AG* motif II in the C-domain, as reported for other *AG* homologs (Kramer et al., 2004). A comparison of deduced amino acid sequence of *FnAG* and *AG* homologs from other woody species showed a highly conserved 56 residue MADS-domain (Fig. 1b). *FnAG* shared greater than 96% amino acid identity to the other *AG* homologs within the MADS-domain. In addition to the MADS-domain, regions including I- and K-domains were also conserved among *FnAG* and other *AG* homologs (Fig. 1b). Overall, *FnAG* was most similar to FpAG from *F. pennsylvanica*, showing 94% identity, followed by 81% identity with GAG2 from *Panax ginseng*, 77% with PtAG2 from *Populus trichocarpa*, 75% with PsAG from *Prunus serotina* and PtAG1, 74% with PpMADS4 from *Prunus persica*, and 68% with *AG* from *Arabidopsis thaliana* and MdAG from *Malus domestica*. A phylogenetic tree was constructed using the deduced amino acid sequence of *FnAG* and 28 other MADS-box proteins (Fig. 2). Phylogenetic analysis placed *FnAG* within the clade of C-lineage *AG* subfamily genes, showing high bootstrap support for a close relationship with SiAG from *Sesamum indicum* and CsAG from *Citrus sinensis*.

3.2. Expression analysis of FnAG in black ash tissues

The spatial expression of *FnAG* was investigated in various vegetative and reproductive tissues using semi-quantitative RT-PCR (Fig. 3a). Gene-specific primers were used to amplify the 183-bp long internal fragment of *FnAG*. Amplification of an *eEFAα* fragment was used as a constitutively expressed gene control to enable inter-sample comparisons. The transcripts of *FnAG* were detected in the female and male flowers and in vitro shoot cultures, but only rarely in leaves. The steady state levels of *FnAG* in reproductive tissues were higher than in in-vitro shoot cultures, showing a higher relative intensity of amplified product. The relative mRNA expression level of *FnAG* was also examined by qPCR (Fig. 3b). The mRNA levels of *FnAG* were 25.8- and 13.5-fold higher in female and male flowers, respectively, than in leaves. Its level in in-vitro shoot cultures was 2.3-fold higher than in leaves.

3.3. Ectopic expression of FnAG in Arabidopsis

We used ectopic expression of *FnAG* CDS in *Arabidopsis* to determine whether *FnAG* could function as *AG*. A binary vector pBI121 containing *35S*::*FnAG* and neomycin phosphotransferase II (*nptII*) gene was introduced into *Arabidopsis* ecotype Col-0 via *Agrobacterium* transformation. Among a total of 17 kanamycin-resistant T_1 plants, the presence of *FnAG* was confirmed from seven independent plants (data not shown) and these were used to generate T_3 plants for phenotyping. Phenotypic alterations were observed in *FnAG*-overexpressing plants (Fig. 4). The most prominent changes in the *FnAG*-overexpressing transgenic plants were the homeotic modifications in the first and second whorls of flowers. Compared to wild-type flowers consisting of four sepals, four petals, six stamens, and a pistil (Fig. 4a), transgenic flowers displayed petals transformed into stamen-like structures (Fig. 4b), and sepals converted into carpel-like structures (Fig. 4c). Third and fourth whorls developed normally, resulting in fertility. The *35S*::*FnAG* plants also showed small and curled leaves (Fig. 4d), immature early flowers with sepals which failed to enclose flower buds (Fig. 4e), and reduced plant size (Fig. 4f). *FnAG*-overexpressing plants flowered significantly earlier than wild-type and empty-vector control plants (Fig. 4g-i).

Based on the flowering time and phenotypic alteration, transgenic

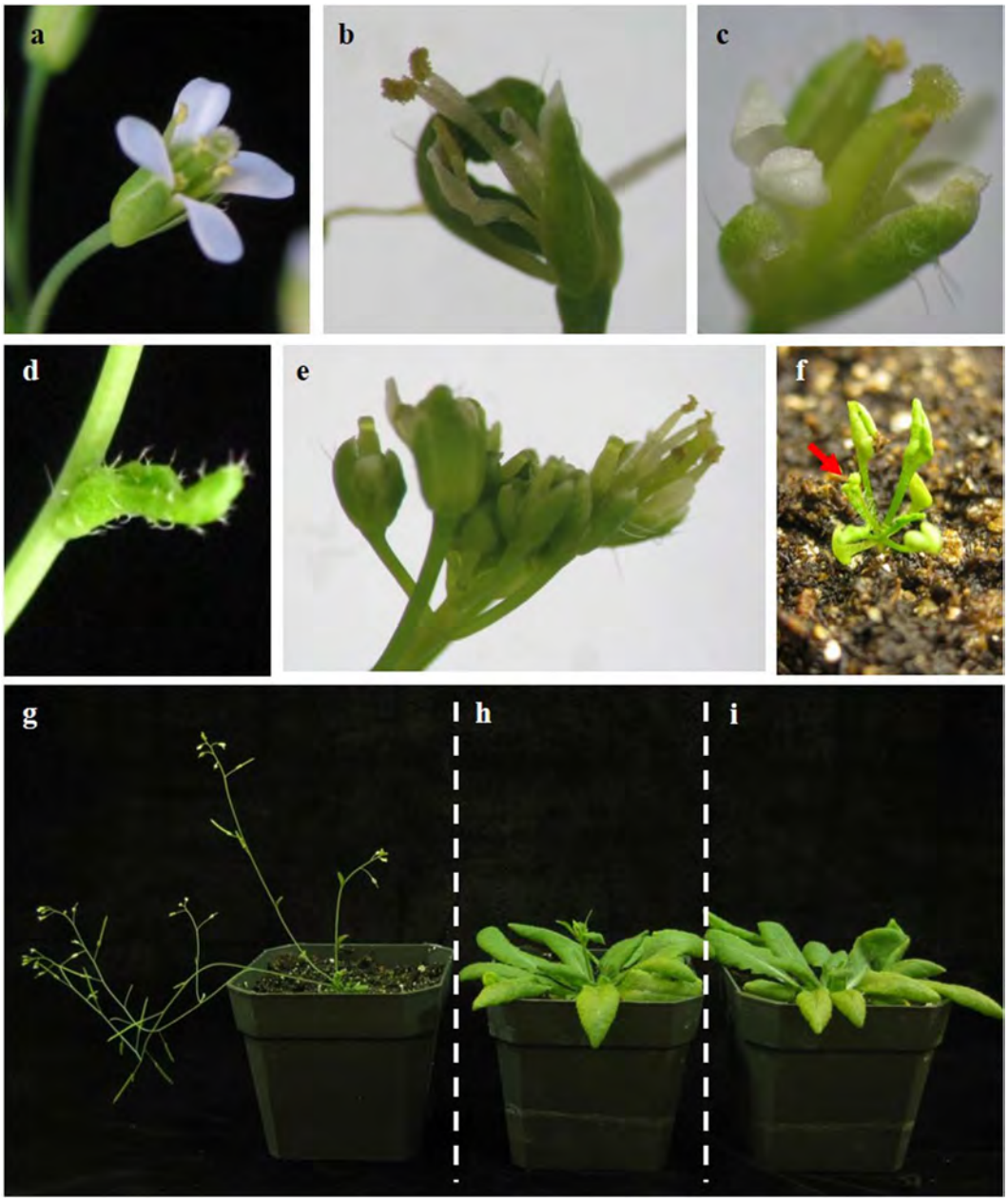

Fig. 4. Floral and vegetative morphology of *Arabidopsis*. (a) Wild-type flower. Transgenic flowers overexpressing *FnAG* under the 35S promoter showed homeotic mutations in the first and second whorls including (b) stamen-like petals, or (c) sepals converted into carpel-like structures. (d) Curled transgenic cauline leaf entrapping the lateral inflorescence. (e) Immature early flowers showing failure of the sepals to enclose flower buds. (f) Extremely small size transgenic plant with early bolting. Arrow indicates floral buds. Thirty-one-day-old (g) transgenic, (h) wild-type, and (i) empty vector control plants.

Fig. 5. Phenotypes of transgenic *Arabidopsis* (*35S::FnAG*) plants with (a) strong or (b) weak phenotypic alterations compared to (c) wild-type plant.

Table 2
Flowering times of wild-type and transgenic *Arabidopsis*.

Genotype	Days to flowering	No. leaves	No. plants
Wild-type (Col-0)	32.79 ± 0.83	14.89 ± 0.78	9
35S::*FnAG* weak	25.96 ± 1.40	10.10 ± 1.07	27
35S::*FnAG* strong	20.17 ± 1.44	5.19 ± 1.51	36

Values represent means ± SD.

plants were classified into two groups (Fig. 5). Although plants with weak *ap2*-like phenotype (Fig. 5b) showed relatively normal vegetative growth compared to strong phenotype plants (Fig. 5a), they displayed smaller plant size than wild-type plants (Fig. 5c). Plants with strong phenotype produced first flowers 12.62 days earlier (with 5.19 rosette leaves) than the wild-type, while plants with weak phenotypic alteration produced first flowers 6.83 days earlier (with 10.1 rosette leaves) than the wild-type (Table 2). The *FnAG* mRNA expression level was higher in the strong phenotype group (#1, #3, #4, and #6) than that in the weak phenotype group (#2, #5, and #7) (Fig. 6a). The endogenous *AtAG* mRNA expression, however, was not significantly different among plants in all groups (Fig. 6b).

4. Discussion

During the diversification of the *AG* subfamily genes in angiosperms, gene duplication and functional evolution have occurred, giving rise to the C- and D-lineage (Kramer et al., 2004). Thus, the D-lineage genes such as *SEEDSTICK* (*STK*; formerly known as *AGL11*) also belong to the *AG* subfamily and were preferentially recruited for ovule development (Dreni and Kater, 2014). Subsequent duplications in the C-lineage have led to paralogous lineages of *PLENA* (*PLE*) from *Antirrhinum* and eu*AG* from *Arabidopsis*, maintaining functional redundancy (Kramer et al., 2004). Although *PLE* C-lineage genes in *Arabidopsis*, such as *SHATTERPROOF1* (*SHP1*) and *SHP2* (formerly known as *AGL1* and *AGL5*, respectively), are similar to *AG* in function, they were not expressed in the meristem and primordial cells at the appropriate time, so *AG* was the only fully functional C-class gene (Dreni and Kater, 2014). In the present study, phylogenetic analysis confirmed that *FnAG* was placed within the eu*AG* C-lineage clade, indicating that *FnAG* was associated with C-function of *AG*.

FnAG showed typical gene structure; the position and number of introns in *FnAG* was conserved with respect to other *AG* homologs (Brunner et al., 2000; Kramer et al., 2004). Unlike other MIKC-type MADS-box genes that have six introns, genes in the C-lineage of *AG* subfamily including *FnAG* have two additional introns positioned 5′ of the MADS domain and in the last codon of *AG* motif II (Kramer et al., 2004). In *FnAG*, the second intron was about 2 kb spanning the largest part of the gene, which might contain functionally important regulatory sequences for controlling its expression specifically to stamens and carpels. Previous studies in *Arabidopsis* demonstrated that the second intron contains cis-regulatory elements that are the binding sites of activators such as LEAFY and WUSCHEL, or repressors such as AP2 or LEUNIG, to control *AG* expression (Sieburth and Meyerowitz, 1997; Deyholos and Sieburth, 2000; Hong et al., 2003). This binding motif was also highly conserved in poplar (Brunner et al., 2000). It has been suggested that using the enhancer element in the second intron of *AG* could produce complete sterility in *Arabidopsis* and tobacco through tissue-specific ablation of stamens and carpels (Liu and Liu, 2008; Wang

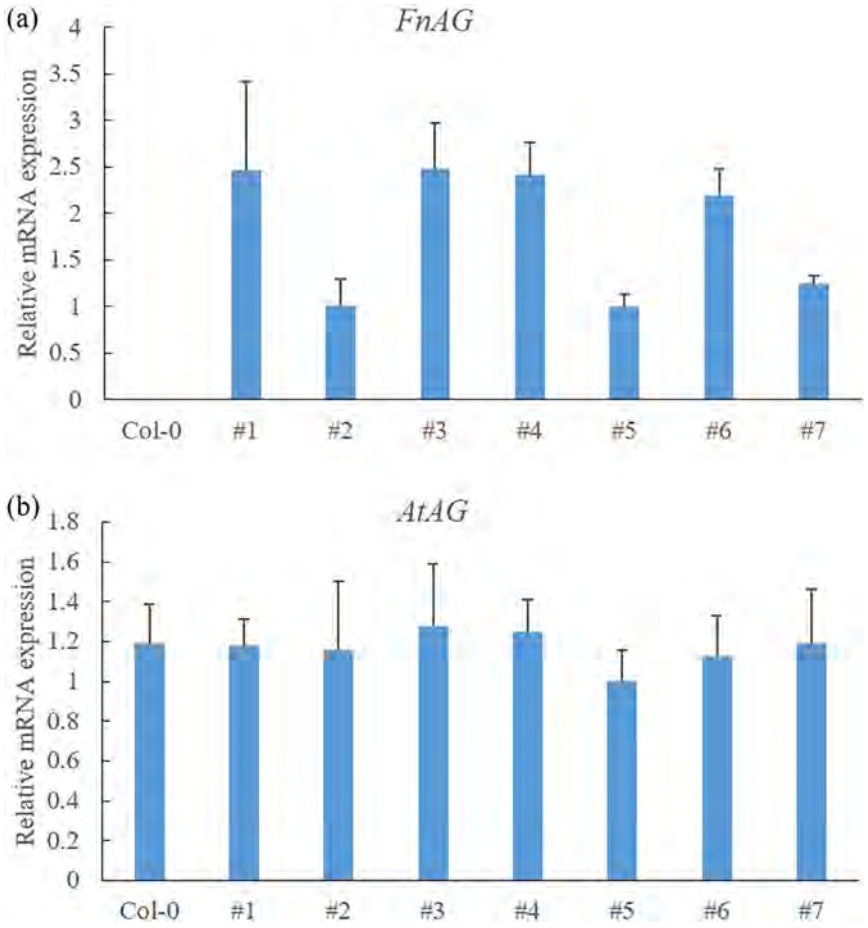

Fig. 6. Relative expression levels of (a) ectopically expressed *FnAG* and (b) endogenous *AtAG* in wild-type (Col-0) and transgenic *Arabidopsis*. Expression levels were normalized to *AtActin2*. Each reaction had three biological replicates and was repeated twice. Error bars represent the standard deviation.

et al., 2008). Although we did not study this regulatory element in detail, this approach would likely be a practical method to achieve gene containment in transgenic trees.

A previous study revealed that there was only one *AG* homolog in green ash (Du and Pijut, 2010). A BLAST search of *FnAG* against the European ash (*F. excelsior*) genome (www.ashgenome.org) showed that European ash may contain two *AG* homologs (personal communication with Richard Buggs, Queen Mary University of London).

The deduced amino acid sequence of *FnAG* revealed extensive sequence similarity with other *AG* proteins. As a major determinant of DNA binding, the MADS-domain was highly conserved in *FnAG*. As was found for *AG* and proteins of *AG* homologs, *FnAG* included an additional peptide extension of 17 amino acid residues at the N-terminal before the MADS domain (Fig. 1b). The N-terminal extension peptide, however, does not appear to affect *AG* activity, because proteins of some *AG* homologs that lack this extension, such as LLAG1 in lily, HpAG in *Hosta plantaginea*, and CiAG in pecan, function normally (Mizukami et al., 1996; Benedito et al., 2004; Wang et al., 2012; Zhang et al., 2016). The I- and K-domains of *FnAG* were moderately conserved, but showed high sequence similarity to those of *FpAG*. According to Pnueli et al. (1994), in this region, tomato showed a closer relationship with tobacco than Brassicaceae, and *Antirrhinum* was more closely related to the Solanaceae than Brassicaceae, suggesting the apparent evolutionary relationship between species in this region.

The C-domain is the most variable region and its function has not yet been elucidated. Studies of truncated *AG* protein lacking the C-domain, however, showed *ag*-like phenotype, indicating that the truncated *AG* protein inhibits normal *AG* function (Mizukami et al., 1996). Complete male sterility was obtained only in transgenic tobacco ectopically expressing truncated PrAG1 protein without the K- and C-domain, but not in lines expressing the full-length protein, indicating that the C domain or C plus K domains may affect the MADS dimer formation between PrAG1 and NAG1 (Liu, 2012). In *Prunus lannesiana*, a 170-bp exon skip caused by abnormal splicing deleted the C-domain *AG* motifs I and II. The result was a double-flowered phenotype in which stamens and carpels were converted to petaloid organs (Liu et al., 2013). Overall, the C-domain is functionally important, and it could be involved in transcriptional activation or higher-order protein interactions for the formation of multimeric transcription factor complexes (Theissen et al., 2000; Kramer et al., 2004).

In addition to evidence from amino acid sequence analyses of *FnAG*, the steady state transcript pattern of *FnAG* strongly indicated that *FnAG* was the ortholog of *AG*. The spatial pattern of transcript abundance for *FnAG*, specifically its abundance in reproductive tissues, corresponded with that of *Arabidopsis AG* and other *AG* homologous genes (Yanofsky et al., 1990; Du and Pijut, 2010; Liu, 2012; Zhang et al., 2013). Although *FnAG* transcripts were also detected in vegetative tissues, as observed in poplar (Brunner et al., 2000) and pecan (Zhang et al., 2016), the steady state levels in vegetative tissue were significantly lower than in reproductive tissues.

In nature, double-flowered mutants provide strong evidence that homeotic mutant phenotypes of this class derive from mutations in *AG* homologous genes. A study with a double-flowered ranunculid mutant 'Double White' revealed that the insertion of a retrotransposon within the putative *AG* ortholog *ThtAG1* caused either nonsense-mediated decay of transcripts or alternative splicing that resulted in mutant proteins with K-domain deletions (Galimba et al., 2012). Loss of C-domain *AG* motifs I and II in *PreAG* caused by abnormal splicing produced the double-flowered cultivar of *Prunus lannesiana* (Liu et al., 2013). Even though there were no significant differences between the double-flowered cultivar and wild-type plants in promoter and intron sequences, the level of *TrimAG* transcript was reduced in the double-flowered *Tricyrtis macranthopsis* cultivar, indicating it might derive from a mutation in one of the genes in the regulatory network that controls *TrimAG* expression or, alternatively, transcriptional silencing by methylation of *TrimAG* promoter/intron sequences (Sharifi et al., 2015).

The function of isolated *AG* homologs usually has been examined by ectopic expression in model plants to see if the transgenic plants showed homeotic alteration. That was because complementation analysis was more difficult, as the null-mutant of *AG* was completely sterile. However, not all *AG* homologous genes cause the typical homeotic alteration of *ap2*-like phenotype in transgenic plants when ectopically overexpressed. The ectopic expression of *NTAG1* from Chinese narcissus rarely produced the homeotic floral phenotype, especially as the generation of transgenic plants increased (Deng et al., 2011). Liu (2012) also found no phenotypic effect on floral development from transgenic tobacco plants with ectopic expression of *PrAG1*. This could be because there were different interacting cofactors in ectopic tissues, or endogenous genes in transformed plants masked the functionality of *AG* homologs from other species (Liu, 2012). The long juvenility of black ash (10–15 years) significantly complicates transgenic evaluation of flowering gene action within the species. Therefore, in the present study, we used *Arabidopsis* for the functional analysis of *FnAG*. The ectopic expression of *FnAG* in transgenic *Arabidopsis* induced homeotic conversions of carpeloid sepals and stamenoid petals, curled leaves, reduced plant size, and prematurely terminated inflorescences, as has been reported for other *AG* homologs (Du and Pijut, 2010; Wang et al., 2012; Liu et al., 2013). The transgenic plants also showed accelerated flowering: 12.62 and 6.83 days earlier in strong and weak phenotypes, respectively, than wild-type. Ectopic expression of the Gm*GAL2*, a soybean *AGAMOUS Like 2*, enhanced flowering in transgenic *Arabidopsis* regardless of the photoperiod by promoting the expression of key flowering genes *CONSTANS* (*CO*) and *FLOWERING LOCUS T* (*FT*), and suppressing floral inhibitor *FLOWERING LOCUS C* (*FLC*) (Xu et al., 2010).

5. Conclusions

In summary, an *AG* ortholog was cloned from black ash and its function in floral organ identity was analyzed. Sequence analysis and expression analysis showed that *FnAG* was closely related to the other *AG* homologs with transcript expression specifically in the reproductive tissues. *FnAG* was involved in floral organ identity, as expected for a functional homolog of *AG* in black ash. Based on these data, we conclude that *FnAG* is a strong candidate for the black ash functional ortholog of *Arabidopsis AG*, and we believe *FnAG* will be an excellent target for genome editing to produce transgenic sterile black ash. Our goal is to manipulate *FnAG* using a targeted genome modification technique -clustered regularly interspaced short palindromic repeats (CRISPR)/CRISPR-associated (Cas) system- for production of sterile black ash. CRISPR/Cas9 constructs targeting *FnAG* are being developed and transformation is currently underway.

Data Archiving Statement

Sequence data for *FnAG* have been archived in GenBank under accession number KX592173.

Acknowledgements

This research was supported by partial funding from the USDA-APHIS-PPQ Center for Plant Health Science and Technology (105703), the U.S. Endowment for Forestry and Communities (108121), and members of the Indiana Hardwood Lumbermen's Association (301648).

Mention of a trademark, proprietary product, or vendor does not constitute a guarantee or warranty of the product by the U.S. Department of Agriculture and does not imply its approval to the exclusion of other products or vendors that also may be suitable.

References

Alvarez-Buylla, E.R., Pelaz, S., Liljegren, S.J., Gold, S.E., Burgeff, C., Ditta, G.S., Ribas de Pouplana, L., Martínez-Castilla, L., Yanofsky, M.F., 2000. An ancestral MADS-box gene duplication occurred before the divergence of plants and animals. Proc. Natl. Acad. Sci. U. S. A. 97, 5328–5333.

Angenent, G.C., Franken, J., Busscher, M., van Dijken, A., van Went, J.L., Dons, H.J., van Tunen, A.J., 1995. A novel class of MADS box genes is involved in ovule development in petunia. Plant Cell 7, 1569–1582.

Beasley, R.R., Pijut, P.M., 2013. Regeneration of plants from *Fraxinus nigra* Marsh. hypocotyls. Hortscience 48, 887–890.

Benedict, M.A., 2001. Black Ash: Its Use by Native Americans, Site Factors Affecting Seedling Abundance and Ring Growth in Northern Minnesota. (MS thesis) Univ. of Minnesota, St. Paul, MN.

Benedito, V.A., Visser, P.B., van Tuyl, J.M., Angenent, G.C., de Vries, S.C., Krens, F.A., 2004. Ectopic expression of *LLAG1*, an *AGAMOUS* homologue from lily (*Lilium longiflorum* Thunb.) causes floral homeotic modifications in *Arabidopsis*. J. Exp. Bot. 55, 1391–1399.

Brunner, A., Li, J., DiFazio, S., Shevchenko, O., Montgomery, B., Mohamed, R., Wei, H., Ma, C., Elias, A., VanWormer, K., Strauss, S., 2007. Genetic containment of forest plantations. Tree Genet. Genomes 3, 75–100.

Brunner, A.M., Rottmann, W.H., Sheppard, L.A., Krutovskii, K., DiFazio, S.P., Leonardi, S., Strauss, S.H., 2000. Structure and expression of duplicate *AGAMOUS* orthologues in poplar. Plant Mol. Biol. 44, 619–634.

Coen, E.S., Meyerowitz, E.M., 1991. The war of the whorls: genetic interactions controlling flower development. Nature 353, 31–37.

Daniell, H., 2002. Molecular strategies for gene containment in transgenic crops. Nat. Biotechnol. 20, 581–586.

Deng, X., Xiong, L., Wang, Y., Sun, Y., Li, X., 2011. Ectopic expression of an *AGAMOUS* homolog *NTAG1* from Chinese narcissus accelerated earlier flowering and senescence in *Arabidopsis*. Mol. Plant Breed. 2, 14–21.

Deyholos, M.K., Sieburth, L.E., 2000. Separable whorl-specific expression and negative regulation by enhancer elements within the *AGAMOUS* second intron. Plant Cell 12, 1799–1810.

Dreni, L., Kater, M.M., 2014. MADS reloaded: evolution of the *AGAMOUS* subfamily genes. New Phytol. 201, 717–732.

Du, N., Pijut, P.M., 2010. Isolation and characterization of an *AGAMOUS* homolog from *Fraxinus pennsylvanica*. Plant Mol. Biol. Report. 28, 344–351.

Galimba, K.D., Tolkin, T.R., Sullivan, A.M., Melzer, R., Theißen, G., Di Stilio, V.S., 2012. Loss of deeply conserved C-class floral homeotic gene function and C- and E-class protein interaction in a double-flowered ranunculid mutant. Proc. Natl. Acad. Sci. 109, E2267–E2275.

Gramzow, L., Ritz, M.S., Theißen, G., 2010. On the origin of MADS-domain transcription factors. Trends Genet. 26, 149–153.

Gucker, C.L., 2005. Fraxinus nigra. In: Fire Effects Information System, [Online]. U.S. Department of Agriculture, Forest Service, Rocky Mountain Research Station, Fire Sciences Laboratory (Producer). (Available: http://www.feis-crs.org/feis/).

Hong, R.L., Hamaguchi, L., Busch, M.A., Weigel, D., 2003. Regulatory elements of the floral homeotic gene *AGAMOUS* identified by phylogenetic footprinting and shadowing. Plant Cell 15, 1296–1309.

Honma, T., Goto, K., 2001. Complexes of MADS-box proteins are sufficient to convert leaves into floral organs. Nature 409, 525–529.

Kovacs, K.F., Mercader, R.J., Haight, R.G., Siegert, N.W., McCullough, D.G., Liebhold, A.M., 2011. The influence of satellite populations of emerald ash borer on projected economic costs in U.S. communities, 2010–2020. J. Environ. Manag. 92, 2170–2181.

Kramer, E.M., Jaramillo, M.A., Di Stilio, V.S., 2004. Patterns of gene duplication and functional evolution during the diversification of the *AGAMOUS* subfamily of MADS box genes in angiosperms. Genetics 166, 1011–1023.

Larkin, M.A., Blackshields, G., Brown, N.P., Chenna, R., McGettigan, P.A., McWilliam, H., Valentin, F., Wallace, I.M., Wilm, A., Lopez, R., Thompson, J.D., Gibson, T.J., Higgins, D.G., 2007. Clustal W and Clustal X version 2.0. Bioinformatics 23, 2947–2948.

Leopold, D.J., McComb, W.C., Muller, R.N., 1998. Trees of the Central Hardwood Forests of North America. Timber Press, Portland, OR.

Liu, J.J., 2012. Ectopic expression of a truncated *Pinus radiata AGAMOUS* homolog (*PrAG1*) causes alteration of inflorescence architecture and male sterility in *Nicotiana tabacum*. Mol. Breed. 30, 453–467.

Liu, X., Anderson, J., Pijut, P.M., 2010. Cloning and characterization of *Prunus serotina AGAMOUS*, a putative flower homeotic gene. Plant Mol. Biol. Report. 28, 193–203.

Liu, Z., Liu, Z., 2008. The second intron of *AGAMOUS* drives carpel- and stamen-specific expression sufficient to induce complete sterility in *Arabidopsis*. Plant Cell Rep. 27, 855–863.

Liu, Z., Zhang, D., Liu, D., Li, F., Lu, H., 2013. Exon skipping of *AGAMOUS* homolog *PrseAG* in developing double flowers of *Prunus lannesiana* (Rosaceae). Plant Cell Rep. 32, 227–237.

Mattanovich, D., Rüker, F., Machado, A.C., Laimer, M., Regner, F., Steinkellner, H., Himmler, G., Katinger, H., 1989. Efficient transformation of *Agrobacterium* spp. by electroporation. Nucleic Acids Res. 17, 6747.

Meyerowitz, E.M., Bowman, J.L., Brockman, L.L., Drews, G.N., Jack, T., Sieburth, L.E., Weigel, D., 1991. A genetic and molecular model for flower development in *Arabidopsis thaliana*. Development 113, 157–167.

Mizukami, Y., Huang, H., Tudor, M., Hu, Y., Ma, H., 1996. Functional domains of the floral regulator AGAMOUS: characterization of the DNA binding domain and analysis of dominant negative mutations. Plant Cell 8, 831–845.

Mizukami, Y., Ma, H., 1992. Ectopic expression of the floral homeotic gene *AGAMOUS* in transgenic *Arabidopsis* plants alters floral organ identity. Cell 71, 119–131.

Murashige, T., Skoog, F., 1962. A revised medium for rapid growth and bioassays with tobacco tissue cultures. Physiol. Plant. 15, 473–497.

Nisbet, D., Kreutzweiser, D., Sibley, P., Scarr, T., 2015. Ecological risks posed by emerald ash borer to riparian forest habitats: a review and problem formulation with management implications. For. Ecol. Manag. 358, 165–173.

Pelaz, S., Ditta, G.S., Baumann, E., Wisman, E., Yanofsky, M.F., 2000. B and C floral organ identity functions require *SEPALLATA* MADS-box genes. Nature 405, 200–203.

Pnueli, L., Hareven, D., Rounsley, S.D., Yanofsky, M.F., Lifschitz, E., 1994. Isolation of the tomato *AGAMOUS* gene *TAG1* and analysis of its homeotic role in transgenic plants. Plant Cell 6, 163–173.

Poland, T.M., McCullough, D.G., 2006. Emerald ash borer: invasion of the urban forest and the threat to North America's ash resource. J. For. 104, 118–124.

Rivera-Vega, L., Mamidala, P., Koch, J.L., Mason, M.E., Mittapalli, O., 2012. Evaluation of reference genes for expression studies in ash (*Fraxinus* spp.). Plant Mol. Biol. Report. 30, 242–245.

SAS® Institute Inc., 2011. SAS® 9.3 Software Package, Cary, NC, USA .

Schwarz-Sommer, Z., Huijser, P., Nacken, W., Saedler, H., Sommer, H., 1990. Genetic control of flower development by homeotic genes in *Antirrhinum majus*. Science 250, 931.

Sharifi, A., Oizumi, K., Kubota, S., Bagheri, A., Shafaroudi, S.M., Nakano, M., Kanno, A., 2015. Double flower formation in *Tricyrtis macranthopsis* is related to low expression of *AGAMOUS* ortholog gene. Sci. Hortic. 193, 337–345.

Sieburth, L.E., Meyerowitz, E.M., 1997. Molecular dissection of the *AGAMOUS* control region shows that cis elements for spatial regulation are located intragenically. Plant Cell 9, 355–365.

Tamura, K., Peterson, D., Peterson, N., Stecher, G., Nei, M., Kumar, S., 2011. MEGA5: molecular evolutionary genetics analysis using maximum likelihood, evolutionary distance, and maximum parsimony methods. Mol. Biol. Evol. 28, 2731–2739.

Theissen, G., Becker, A., Rosa, A.D., Kanno, A., Kim, J.T., Münster, T., Winter, K.-U., Saedler, H., 2000. A short history of MADS-box genes in plants. Plant Mol. Biol. 42, 115–149.

van Frankenhuyzen, K., Beardmore, T., 2004. Current status and environmental impact of transgenic forest trees. Can. J. For. Res. 34, 1163–1180.

Wang, H.Z., Hu, B., Chen, G.P., Shi, N.N., Zhao, Y., Yin, Q.C., Liu, J.J., 2008. Application of *Arabidopsis AGAMOUS* second intron for the engineered ablation of flower development in transgenic tobacco. Plant Cell Rep. 27, 251–259.

Wang, Y., Zhang, X., Liu, Z., Zhang, D., Wang, J., Liu, D., Li, F., Lu, H., 2012. Isolation and characterization of an *AGAMOUS*-like gene from *Hosta plantaginea*. Mol. Biol. Rep. 39, 2875–2881.

Xu, J., Zhong, X., Zhang, Q., Li, H., 2010. Overexpression of the Gm*GAL2* gene accelerates flowering in *Arabidopsis*. Plant Mol. Biol. Report. 28, 704–711.

Yanofsky, M.F., Ma, H., Bowman, J.L., Drews, G.N., Feldmann, K.A., Meyerowitz, E.M., 1990. The protein encoded by the *Arabidopsis* homeotic gene *AGAMOUS* resembles transcription factors. Nature 346, 35–39.

Zhang, X., Henriques, R., Lin, S.-S., Niu, Q.-W., Chua, N.-H., 2006. *Agrobacterium*-mediated transformation of *Arabidopsis thaliana* using the floral dip method. Nat. Protoc. 1, 641–646.

Zhang, J., Li, Z., Guo, C., Liu, G., Bao, M., 2013. Isolation and functional analyses of a putative floral homeotic C-function gene in a basal eudicot London plane tree (*Platanus acerifolia*). PLoS One 8, e63389.

Zhang, J., Wang, M., Mo, Z., Wang, G., Guo, Z., 2016. Molecular characterization and functional analysis of an *AGAMOUS*-like gene *CiAG* from pecan. Hortscience 51, 664–668.